

Evaluation of Stress Distribution Due to Shearing in Non-Oriented Electrical Steel by Synchrotron Radiation and Effect of Grain Size on Iron Loss Deterioration Due to Shearing

ZAIZEN Yoshiaki^{*1} OMURA Takeshi^{*2} TODA Hiroaki^{*3}

Abstract:

The influence of shearing process on the iron loss of non-oriented electrical steels with grain sizes of 10 μm to 150 μm was investigated. The deterioration ratio of iron loss was clearly smaller in sample with small grain sizes. The shear droop height, reflecting the amount of plastic deformation, displayed a good correlation with the deterioration of iron loss under the effect of the material grain size. To clarify the strain distribution around the sheared edge, elastic-plastic strain in a sheet sample with the thickness of 0.30 mm and grain size of 10 μm was evaluated by using synchrotron radiation. The width of the region of elastic strain due to shearing was two or three times of the material thickness. The results of the elastic-plastic strain distribution obtained by measurements were then used to estimate the iron loss deterioration rate in 5 mm width sheared samples. The estimated loss deterioration coincided with the actual measured iron loss.

1. Introduction

Non-oriented electrical steel is widely used as a core material for motors, generators and other electrical equipment, and is an important soft magnetic material which supports today's society. In recent years, requirements for higher efficiency and energy saving in motors have become increasingly strict from the viewpoint of high efficiency in energy use, and higher performance has also been demanded in non-oriented electrical steel. Moreover, in order to achieve high performance and high efficiency in motors, appropriate selection of

materials for cores corresponding to their distinctive features and optimum material use are also considered necessary¹⁻³⁾.

Although motor cores are generally manufactured by punching non-oriented electrical steel sheets, it is known that the magnetic properties of electrical steel sheets are deteriorated by the plastic strain and elastic strain that occur around the punched edge in the punching process⁴⁻⁸⁾. The magnetic properties of non-oriented electrical steel sheets are generally measured and evaluated after shearing the material to obtain an Epstein test piece with a width of 30 mm and length of 280 mm conforming to JIS C 2552. In many cases, however, the stator tooth width and yoke width in actual motors are narrower than 30 mm. In particular, due to the orientation toward downsizing of the traction motors of hybrid electric vehicles (HEV) and electric vehicles (EV) in recent years, the ratio of the punched part to the core volume has increased as the stator tooth width and yoke width have become smaller, and as a result, the effect of punching strain has become more apparent. Moreover, because material-related factors (e.g., Si content, sheet thickness, grain size) have a large influence on the magnetic properties of non-oriented electrical steel, it is important to clarify the effects of the material factors in the base material on increased iron loss in the punching process. JFE Steel has clarified those effects, focusing on the Si content and sheet thickness of the materials⁹⁻¹¹⁾.

Although it is necessary to clarify the strain distribution around the punched edge in order to clarify the effects of the punching process on magnetic properties,

[†] Originally published in *JFE GIHO* No. 52 (Aug. 2023), p. 27–33

^{*1} Senior Researcher Manager, Electrical Steel Research Dept., Steel Res. Lab., JFE Steel

^{*2} Senior Researcher Deputy General Manager, Electrical Steel Research Dept., Steel Res. Lab., JFE Steel

^{*3} Dr. Eng., Staff Deputy General Manager, Electrical Steel Business Planning Dept., JFE Steel

few reports have addressed this issue^{5,12}). Therefore, JFE Steel carried out strain measurements by using synchrotron radiation, which enables nondestructive measurement of strain around the punched edge. Because strain measurement utilizing synchrotron radiation is difficult if the sample does not have a small grain size, this paper reports the results of a study¹³) of the influence of grain size on iron loss deterioration in non-oriented electrical steel by a shearing process, which was used to simulate the punching process, and also reports the results of measurements of the strain distribution by synchrotron radiation, focusing on a material with a small grain size¹⁴).

2. Influence of Grain Size of Non-Oriented Electrical Steel on Iron Loss Deterioration in Shearing Process

2.1 Experimental Method

Although motor cores are generally manufactured by punching, here, the samples were prepared by a shearing process simulating punching. In this study, materials with a sheet thickness of 0.30 mm and grain sizes of 10 μm to 155 μm (Vickers hardness HV 0.5: 205 in all cases) were prepared from Si 3.5 mass% material.

As shown in **Fig. 1**, samples with a width of 30 mm and 5 mm were taken from the rolling direction (L direction) and direction perpendicular to the rolling direction (C direction) by shearing with a clearance of 15 μm . The 5 mm width samples were taped together with cellophane tape to form a sample with a width of 30 mm, after which magnetic measurements were carried out by the Epstein test method, and iron loss ($W_{15/50}$) was evaluated by the average value of the L direction and C direction specimens. $W_{15/50}$ means the iron loss when a material is excited at a frequency of 50 Hz and maximum magnetic flux density of 1.5 T. The deterioration ratio of iron loss $\Delta W(\%)$ by shearing was calculated by the following Eq. (1) using the iron loss $W(30\text{ mm})$ of the 30 mm width sample and $W(5\text{ mm})$ of the 5 mm width sample.

$$\Delta W(\%) = \{W(5\text{ mm}) - W(30\text{ mm})\} / W(30\text{ mm}) \times 100 \quad \dots (1)$$

2.2 Experimental Results and Discussion

Figure 2 shows the influence of the material grain size on the deterioration ratio of iron loss ($W_{15/50}$). It can be understood that the deterioration ratio of iron loss shows a good correlation with the grain size and is smaller in samples with smaller grain sizes. Figure 2 is organized by the square root of grain size, which shows

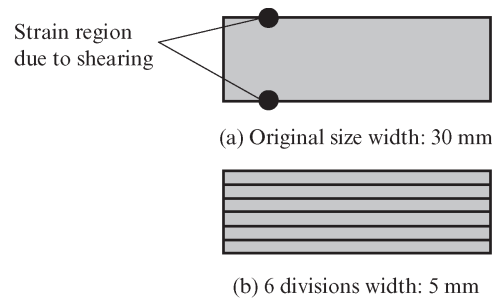


Fig. 1 Schematic view of shearing

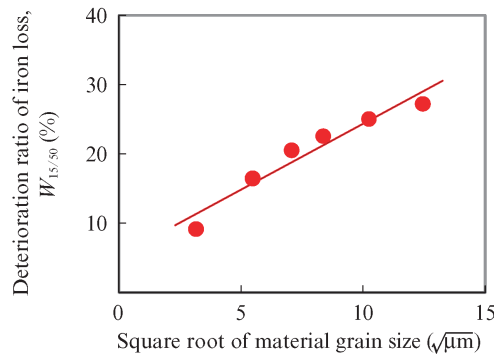


Fig. 2 Influence of material grain size on deterioration of iron loss

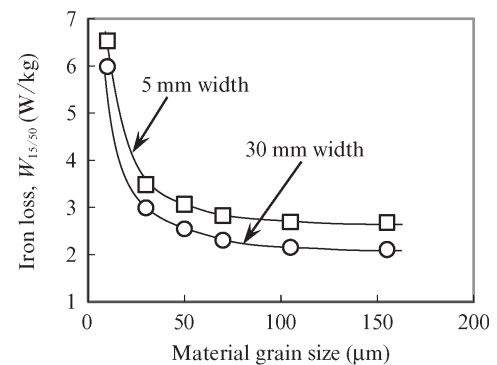


Fig. 3 Influence of material grain size on deterioration of iron loss

a good correlation with the deterioration ratio of iron loss. **Figure 3** shows a comparison of the grain size dependency of iron loss during shearing of the samples with widths of 5 mm and 30 mm. The 30 mm width Epstein test pieces showed the minimum iron loss at the grain size of 15 μm , and the 5 mm width Epstein test pieces also displayed a similar tendency. Although the results in Fig. 2, indicate that it is possible to suppress iron loss deterioration by shearing by reducing the grain size of the material, the absolute value of iron loss in the 50 Hz to 400 Hz region increases when the grain size is reduced. From this viewpoint, it is considered necessary to select materials in consideration of the actual drive conditions of the motor, *etc.*

To investigate the influence of grain size on iron loss

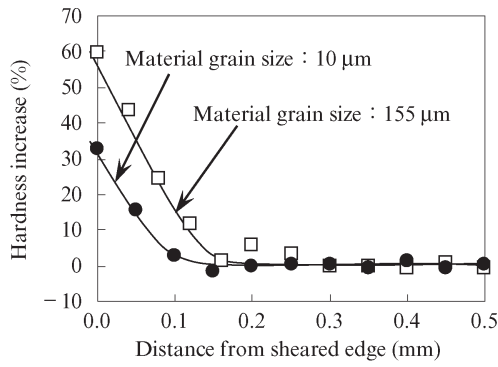


Fig. 4 Influence of material grain size on distribution of hardness increase near sheared edge

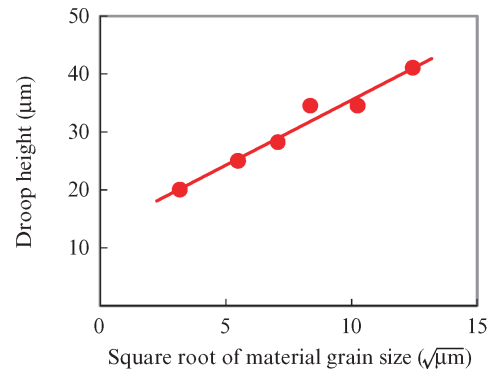
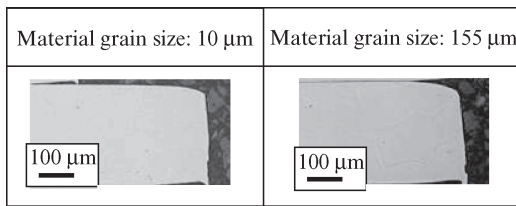
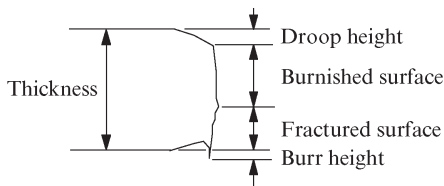


Fig. 6 Influence of material grain size on drop height



(a) Optical micrograph images of cross section near sheared edge



(b) Schematic view of cross section of sheared edge

Fig. 5 Optical micrograph and schematic view of sheared edge

deterioration, the hardness distribution of the sheared edge was measured with a micro Vicker hardness tester, and the obtained hardness distribution was evaluated by the hardness increase ratio (%) in comparison with the area that was unaffected by shearing. **Figure 4** shows the results of an investigation of the hardness distribution of the sheared edge of samples with different grain sizes of the original material (grain size: 10 μm, 155 μm, HV 0.5: 205, sheet thickness: 0.30 mm). Since the region of hardness increase around the sheared edge was larger in the material with the larger grain size, it could be inferred that the amount of plastic deformation due to shearing was larger. Therefore, the droop height of the sheared edge was measured. **Figure 5** shows an example of the results of cross-sectional observation of the sheared edge (grain size: 10 μm and 155 μm materials) and a schematic diagram of the shape of the sheared edge. **Figure 6** shows the influence of the grain size on the droop height defined in Fig. 5, and indicates that droop height of the sheared edge was larger in the material with the larger

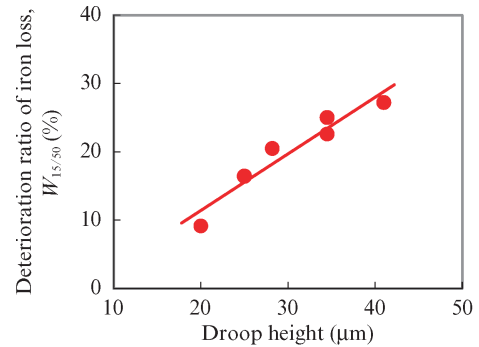


Fig. 7 Influence of drop height on deterioration of iron loss

grain size.

Because the relative size of the droop height is considered to represent the relative size of plastic deformation by shearing, the relationship between the droop height and the deterioration ratio of iron loss $\Delta W(\%)$ was investigated. The results are shown in **Fig. 7**. These results show that there is an extremely good correlation between the grain size of the material and the deterioration ratio of iron loss by narrow-width shearing. Accordingly, the magnitude of strain introduced by shearing processing can be evaluated from the droop height. Moreover, it is also thought that the deterioration ratio of iron loss decreases because the amount of strain introduced around the sheared edge is reduced by refinement of the material grain size. Here, it may be noted that the width of the region of hardness increase at the sheared edge is approximately one-half of the sheet thickness. While it is thought that plastic strain accumulates in this range^{6,8)}, it has been reported that the change in the magnetic domain structure due to punching or shearing occurs up to about 2 times the sheet thickness, and a region, where elastic strain, which affects material properties, is introduced from the region where plastic strain is accumulated to the inner side of the sheet^{6,8)}. As possible reasons for the good correlation between the droop height of the sheared edge and the deterioration ratio of iron loss in

spite of this strain distribution, it can be thought that the influence of plastic strain on iron loss deterioration may be predominant, or the size of the plastic strain introduced by punching/shearing may also be reflected in the size of the elastic strain.

Therefore, a stress analysis of the shearing process was carried out by the finite element method (FEM) to determine whether the size of plastic strain introduced by processing is reflected in the size of the elastic strain.

2.3 FEM Analysis Conditions

To estimate the stress state introduced in steel sheets by the shearing process, an analysis of some samples with different grain sizes (grain size: 10 μm , 50 μm , 155 μm , HV 0.5: 205, sheet thickness: 0.30 mm) was carried out with 2-dimensional plane-strain elastic-plastic body model using the explicit dynamic finite element simulation software LS-DYNA.

The stress-strain (S-S) curves and ductile fracture parameters of the materials used in the analysis were calculated by the method described below. First, for the S-S curves, in the region of smaller strain from the maximum loading point, the measured values of stress and strain were converted to true stress and true strain, and a multipoint approximation was made. The high strain region was identified by performing a calculation simulating the tensile test by analysis and curve fitting by the measured S-S curve in which the load decreased. For the ductile fracture parameters, the optimum ductile fracture parameters were decided so as to reproduce the droop height of each steel sheet obtained in the experiment by a simulation of the shearing process, using the ductile fracture criteria proposed by Cockcroft et al.¹⁵⁾.

Figure 8 is a schematic diagram showing the initial condition of the stress analysis. The shape of the tool edges is a pin angle. The friction condition between the material and tools was set at $\mu = 0.3$ using Coulomb's law of friction, and the clearance and sheet holding force of the punch and die were set to the same values as in the experiment.

2.4 FEM Analysis Results and Discussion

Figure 9 shows the calculation results of the distribution of stress perpendicular to the page for a sample with a grain size of 50 μm , Vickers hardness HV 0.5 of 205 and sheet thickness of 0.30 mm. Although the stress in the vicinity of the punched edge is tensile stress, this changes to compressive stress from the edge to the interior, and in the region about 0.30 mm or more from the edge, that is, at a distance approximately equal to the sheet thickness, the absolute value of stress is small and approaches zero stress.

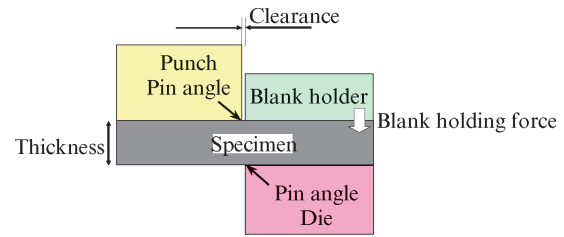


Fig. 8 Stress analysis condition by FEM in shearing process

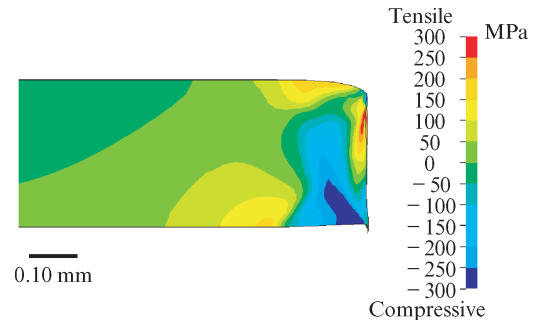


Fig. 9 Distribution of stress perpendicular to the page by FEM calculation for grain size 50 μm sample (Thickness: 0.30 mm, Hardness HV 205)

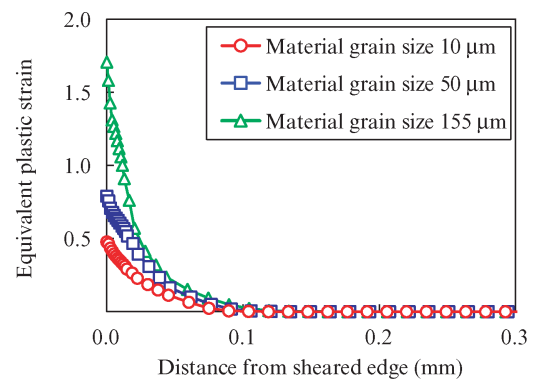


Fig. 10 Influence of material grain size on equivalent plastic strain along centerline in thickness direction by FEM calculation (Thickness: 0.30 mm, Hardness HV 205)

Figure 10 shows the analysis results of the equivalent plastic strain along the centerline in the thickness direction (hereinafter, centerline). As the grain size becomes smaller, the equivalent plastic strain around the sheared edge decreases. On the other hand, in all cases, the position where the equivalent plastic strain becomes zero, that is, the plastic strain region, is the region approximately 0.1 mm from the sheared edge, and grain size dependence is not observed at the centerline. This calculation result is in good agreement with the results of measurements of the hardness increase ratio of the sheared edge shown in Fig. 4. Therefore, this analysis is considered to have sufficient accuracy, to a certain degree, in evaluations of the size of strain, and in turn, the size of strain introduced by processing with a shearing machine.

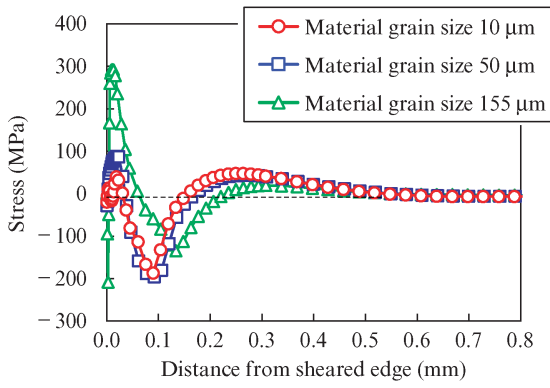


Fig. 11 Influence of material grain size on stress distribution, as shown in Fig. 9, along center line in thickness direction by FEM calculation (Thickness: 0.30 mm, Hardness HV 205)

Figure 11 shows the results of a stress distribution analysis in the direction perpendicular to the page at the material centerline. Comparing the stress values in the plastic deformation region from the sheared edge to a point 0.1 mm from the edge, the tensile stress generated around the sheared edge is smaller in the materials with smaller grain sizes, and tensile stress changes to compressive stress in the region within 0.1 mm from the edge. Moreover, the peak position on the compressive stress side tended to be further from the sheared edge in the sample with the large grain size. On the other hand, according to these results, the position where tensile stress becomes zero was approximately 0.5 mm from the sheared edge in all cases, and the influence of grain size was not observed at the centerline, even in the region where elastic strain was introduced, similar to the plastic region in Fig. 11.

As described above, as a result of a shearing analysis considering differences in the droop height due to grain size, it became clear that the equivalent plastic strain is large when the droop height is large, and compressive stress extends to a distance from the sheared edge. It is known that, in general, iron loss in electrical steel sheets is strongly influenced by plastic strain and compressive stress⁶⁾. Therefore, it is thought that iron loss deterioration during processing is large in materials with large grain sizes because equivalent plastic strain increases by way of the droop height caused by processing, and compressive stress exists to a distance from the processed edge.

3. Evaluation of Strain Distribution by Shearing Process by Synchrotron Radiation

3.1 Experimental Method

An evaluation by synchrotron radiation was carried

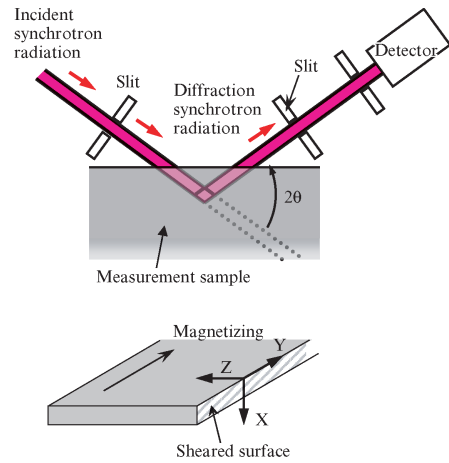


Fig. 12 Strain distribution measurement method by synchrotron radiation

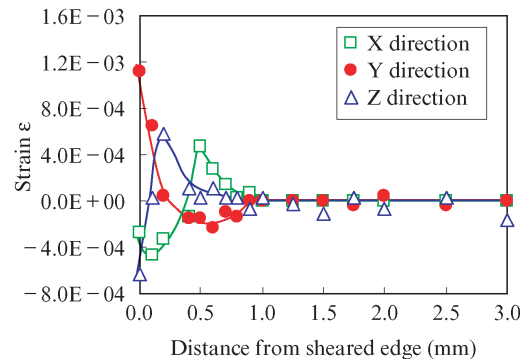


Fig. 13 Strain distribution by shearing process using synchrotron radiation

out to clarify the strain distribution that occurs around the sheared edge as a result of the shearing process. Specimens with a grain size of 10 μm were used to obtain diffraction profiles by synchrotron radiation. The diffraction profile at the center-of-thickness of the sheared edge was measured by the strain scanning-transmission method, as shown in **Fig. 12**. The measurement was performed with ±5 mm diversion in the Y direction to increase the number of grains measured.

3.2 Experimental Results and Discussion

Figure 13 shows the results of a measurement of the strain distribution in the center-of-thickness layer. The region of plastic-elastic strain introduced by shearing extended to about 2 to 3 times the sheet thickness. **Figure 14** shows the results of a calculation of the stress distribution from the strain distribution obtained by synchrotron radiation. Here, the results of the FEM analysis described in section 2.4 and the results of the measurement by synchrotron radiation will be compared. Since the measurement results of the stress distribution in the Y direction obtained by the synchro-

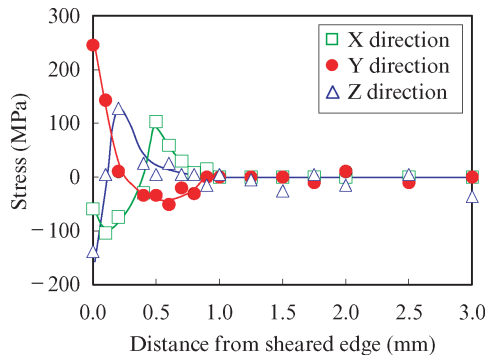


Fig. 14 Stress distribution by shearing process using synchrotron radiation

tron radiation measurement correspond to the FEM analysis results shown in Fig. 11 (grain size: $10\ \mu\text{m}$), those results were compared with the strain distribution in the Y direction in Fig. 14. First, focusing on the region of strain introduction from the sheared edge, in the FEM analysis, the elastic-plastic strain region extended to around 0.5 mm to 0.6 mm from the sheared edge. In contrast, the synchrotron radiation measurement results showed that the elastic-plastic strain region extended to around 0.8 mm to 0.9 mm from the sheared edge. Next, looking at the stress values from the sheared edge, in the FEM analysis, the stress is tensile stress with a maximum value of around 50 MPa in the region 0.05 mm from the sheared edge. This changes to compressive stress with a maximum value of about 200 MPa in the region from 0.05 mm to 0.15 mm, and then to tensile stress of about 50 MPa in the region from 0.15 mm to 0.5 mm. On the other hand, the synchrotron radiation evaluation results show tensile stress with a maximum of approximately 250 MPa in the region from the sheared edge to 0.2 mm, and compressive stress with a maximum of about 40 MPa in the region from 0.2 mm to 0.9 mm. Based on these facts, the results of the comparison of the FEM analysis and the actual measured values showed approximate agreement of the region of elastic-plastic strain introduced from the sheared edge, and agreement on the point that stress changes from compressive to tensile stress. However, since there is some divergence between the stress values, in the future, it will be necessary to improve analytical accuracy when discussing the elastic stress that occurs as a result of processing.

Figure 15 shows a schematic diagram of the strain distribution of the sheared edge. From the results of measurement of the strain distribution by synchrotron radiation in Fig. 13 and the results of measurement of the hardness increase shown in Fig. 4, it is thought that magnetic properties are influenced by plastic strain in the region from the sheared edge to 0.20 mm or less

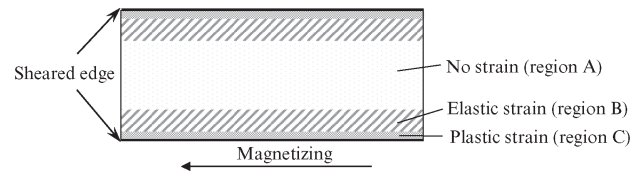


Fig. 15 Schematic diagram of strain distribution by shearing

(called region C), and by elastic strain in the region between 0.20 mm and 1.0 mm (called region B). Strain was not observed in the region more than 1 mm from the sheared edge (called region A).

The deterioration ratio of iron loss for the case of a shearing width of 5 mm was calculated from the elastic-plastic strain distribution results obtained by synchrotron radiation. The average value of the plastic strain region (region C) and the elastic strain region (region B) was calculated from the strain distribution measurement results in Fig. 13, focusing on the strain distribution in the Y direction, which is the same as the magnetization direction of the material, and magnetic properties were measured after applying elastic-plastic strain equivalent to the average value. For the no strain region (region A), the magnetic properties of a sample were measured after strain relief annealing. **Figure 16** (a) shows the magnetization properties in the plastic strain region, elastic strain region and no strain region. When the sample material was sheared with a 5-mm width, and the ratio of each region was calculated from the measured strain distribution, the ratios of the regions were no strain region (region A): 60%, elastic strain region (region B): 32% and plastic strain region (region C): 8%. If the excitation magnetic flux density of each region when a sample sheared to a 5 mm width is excited to the maximum magnetic flux density of 1.5 T is estimated referring to these ratios, the calculation results are no strain region: 1.55 T, elastic strain region: 1.49 T and plastic strain region: 1.12 T. This represents a condition in which the magnetic permeability of regions where strain is introduced by the shearing process decreases greatly, and the magnetic flux concentrates in the region where no strain exists.

Fig. 16 (b) shows the iron loss properties of the plastic strain region, elastic strain region and no strain region. A trial calculation of the iron loss for a 5-mm sheared width was carried out based on the relationship between iron loss and the excitation magnetic flux density in each region in Fig. 16 (b), and the deterioration ratio of iron loss $\Delta W_{15/50}$ was obtained. **Figure 17** shows the calculation results of the deterioration ratio of iron loss. From the results, the calculated deterioration ratio of iron loss was substantially in agreement with the measured deterioration ratio. Based on the above, it was suggested that motor iron loss can be estimated by

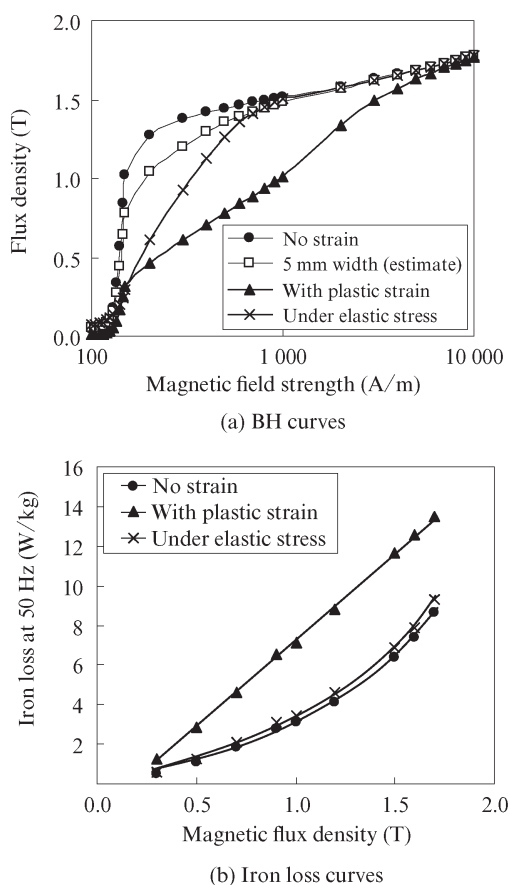


Fig. 16 Comparison of magnetic properties under plastic strain and elastic stress

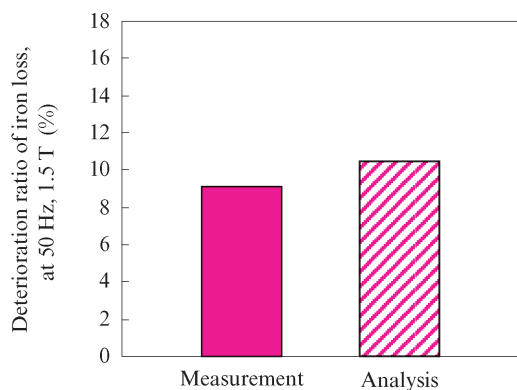


Fig. 17 Comparison of measurement and analysis of iron loss deterioration

evaluating the plastic strain region and elastic strain region of materials.

4. Conclusion

In this paper, the influence of grain size on iron loss deterioration in the shearing process of non-oriented electrical steel was investigated, and the strain distribution in the shearing process was measured by synchrotron radiation. Based on the results, the following

points were clarified.

- (1) The deterioration ratio of iron loss during shearing is smaller in materials with smaller grain sizes. However, because the absolute value of iron loss in the 50 Hz to 400 Hz region increases in materials with small grain sizes, appropriate selection of materials considering the actual driving conditions of a motor, *etc.* is important.
- (2) The deterioration ratio of iron loss due to shearing shows a good correlation with the droop height of the sheared edge. When the droop height is small, plastic strain is small, and the compressive stress field extending from the sheared edge is narrow. It is thought that deterioration of iron loss due to processing is small in materials with small grain sizes for this reason.
- (3) As a result of measurement of the strain distribution at the sheared edge by synchrotron radiation, elastic strain due to shearing occurs in a region with a width 2 to 3 times larger than the sheet thickness.
- (4) A comparison of the stress distribution obtained by an FEM analysis and the stress distribution measured by synchrotron radiation showed that the elastic-plastic strain regions introduced from the sheared edge were approximately in agreement, but some divergence occurred in the stress values.
- (5) When the iron loss deterioration ratio of samples sheared to a width of 5 mm was estimated from the results of the elastic-plastic strain distribution obtained by measurements using synchrotron radiation, the estimated results coincided with the deterioration ratio obtained by actual measurement.

References

- 1) Honda, A.; Kawano, M.; Ishida, M.; Sato, K.; Komatsubara, M. Efficiency of model induction motor using various non-oriented electrical steels. *J. Mater. Sci. Technol.* 2000, vol. 16, no. 2, p. 238–243.
- 2) Toda, H.; Senda, K.; Ishida, M. Effect of material properties on motor iron loss in PM brushless dc motor. *IEEE Trans. Magn.* 2005, vol. 41, no. 10, p. 3937–3939.
- 3) Toda, H.; Senda, K.; Morimoto, S.; Hiratani, T. Influence of various non-oriented electrical steels on motor efficiency and iron Loss in switched reluctance motor. *IEEE Trans. Magn.* 2013, vol. 49, no. 7, p. 3850–3853.
- 4) Schoppa, A.; Schneider, J.; Wuppermann, C. D. Influence of the manufacturing process on the magnetic properties of non-oriented electrical steels. *J. Magn. Magn. Mater.* 2000, vol. 215–216, p. 74–78.
- 5) Rygal, R.; Moses, A. J.; Derebasi, N.; Schneider, J.; Schoppa, A. Influence of cutting stress on magnetic field and flux density distribution in non-oriented electrical steel sheets. *J. Magn. Magn. Mater.* 2000, vol. 215–216, p. 687–689.
- 6) Senda, K.; Ishida, M.; Nakasu Y.; Yagi, M. “Effect of Shearing Process on Iron Loss and Domain Structure of Non-oriented Electrical Steel.” *IEEJ Trans. FM.* 2005, vol. 125, p. 241–246. (Japanese)
- 7) Kurosaki, Y.; Mogi, H.; Fujii, H.; Kubota, T.; Shinozaki, M. Importance of punching and workability in non-oriented electrical steel sheets. *J. Magn. Magn. Mater.* 2008, vol. 320, p. 2474–

- 2480.
- 8) Kaido, C.; Mogi, H.; Fujikura, M.; Yamasaki, J. Punching Deterioration Mechanism of Magnetic Properties of Cores. *IEEJ Trans. FM.* 2008, vol. 128, no. 8, p. 545–550.
 - 9) Toda, H.; Oda, Y.; Zaizen, Y.; *JFE Technical Report.* 2015, no. 36, p. 24–31.
 - 10) Toda, H.; Zaizen, Y.; Namikawa, M.; Shiga, N.; Oda, Y.; Moto-moto, S. Iron loss deterioration by shearing process in non-oriented electrical steel with different thicknesses and its influence on estimation of motor iron loss. *IEEJ Journal of Industry Applications.* 2014, vol. 3, p. 55–61.
 - 11) Omura, T.; Zaizen, Y.; Fukumura, M.; Senda, K.; Toda, H. Effect of Hardness and Thickness of Non-oriented Electrical Steel Sheets on Iron Loss Deterioration by Shearing Process. *IEEE Trans. Magn.* 2015, vol. 51, ID 2005604.
 - 12) Rygal, R.; Moses, A. J.; Derebasi, N.; Schneider, J.; Schoppa, A. Influence of cutting stress on magnetic field and flux density distribution in non-oriented electrical steel sheets. *J. Magn. Magn. Mater.* 2000, vol. 215–216, p. 687–689.
 - 13) Zaizen, Y.; Omura, T.; Senda, K.; Fukumura, M.; Toda, H. *IEEJ Trans. FM.* 2018, vol. 138, no. 11, p. 576–581. (Japanese)
 - 14) Zaizen, Y.; Omura, T.; Fukumura, M.; Senda, K.; Toda, H. Evaluation of stress distribution due to shearing in non-oriented electrical steel by using synchrotron radiation. *AIP Advances* 6. 2016, 055926.
 - 15) Cockcroft, M. G.; Latham, D. J. Ductility and the workability of metals. *Journal of the institute of metal.* 1968, vol. 96, p. 33–39.